Joint International Topical Meeting on Mathematics & Computation and Supercomputing in Nuclear Applications (M&C + SNA 2007)
Monterey, California, April 15-19, 2007, on CD-ROM, American Nuclear Society, LaGrange Park, IL (2007)

THE USE OF MONTE CARLO SIMULATION IN IMPROVING RECONSTRUCTION QUALITY IN SINGLE PHOTON EMISSION COMPUTED TOMOGRAPHY

Mingshan Sun
Department of Nuclear Engineering
University of California, Berkeley, CA 94720
and Department of Radiology
University of California, San Francisco, CA 94107
m_sun@berkeley.edu

Jasmina L Vujic
Department of Nuclear Engineering
University of California, Berkeley, CA 94720
vujic@nuc.berkeley.edu

Bruce H Hasegawa
Department of Nuclear Engineering
University of California, Berkeley, CA 94720
and Department of Radiology
University of California, San Francisco, CA 94107
bruce.hasegawa@radiology.ucsf.edu

ABSTRACT

This paper describes an efficient method of generating a model-based system matrix using Monte Carlo simulation for incorporation into reconstruction algorithms for pinhole SPECT imaging and reconstructions. The method is able to model the imaging geometry for pinhole collimators and the detector depth of interaction effect accurately and efficiently, and has demonstrated improvement in the quality of images reconstructed for small animal imaging.

Key Words: SPECT, Monte Carlo, system matrix, reconstruction, small animal imaging

1. INTRODUCTION

Radionuclide imaging is widely used in both clinical and preclinical studies where a subject is injected with a trace amount of radioactive material that is bound chemically to biologically-active molecules. The imaging study then is performed to measure the distribution and concentration of the radioactive material in the body, from which biological function and metabolic information can be inferred.

Single photon emission computed tomography (SPECT) is a widely used radionuclide imaging technique for medical diagnosis. It detects and counts individual γ-rays emitted from the internally administered radiopharmaceutical using position sensitive γ-ray detectors. It also records

the direction of the detected photons using a collimator which limits the angles across which the photon can be received by the detector. Both parallel-hole and pinhole collimators are common, with the former used clinically to image large parts of the human body, whereas the latter is used to image thyroids or other small organs in humans, or to obtain submillimeter spatial resolution for imaging organs in mice, rats, and other small animals.[1]

Scientific advances in genetics, molecular biology, and pharmacology have increased interest in preclinical experiments where biological processes including disease can be studied in small animals. These studies are now often performed with mice and rats, which are biologically and physiologically similar to humans thus suitable for basic biological research and pharmaceutical discovery and evaluation. They also are small in size, easy to handle and house, are relatively low in cost, and more importantly, are easy to manipulate genetically because their genome is known and because they have a fast reproductive rate. Small animal models of human diseases, including those developed by knock-out and transgenic manipulations, now are widely available and have become critical elements of modern biological research.[2]

Traditionally, radiotracer studies for evaluating physiological function in small animals have been performed using invasive methods such as tissue sampling or autoradiography where the animal does not survive the experimental measurement. Over the past 5 years, "microSPECT" imaging with radionuclide detectors equipped with pinhole collimators has been developed to perform noninvasive *in vivo* imaging with millimeter or submillimeter spatial resolution needed for resolving small organs and small foci of radionuclide uptake.[3, 4] As such, the individual animal is allowed to survive the measurement and serve as its own control. Noninvasive *in vivo* imaging also is important for assessing diagnostic and therapeutic interventions that require longitudinal experiments where measurements are derived from an individual animal over multiple time points.

The advantage of pinhole collimator is that it balances detection efficiency and spatial resolution for imaging small objects. The diameter of the pinhole aperture, typically in the range of 0.5 to 2 mm for small animal imaging, must be selected carefully. Large pinhole sizes allow the image data to be acquired with excellent sensitivity, but have relative poor spatial resolution. Improved spatial resolution can be obtained with smaller sized pinholes, at the cost of decreased sensitivity which in turn lengthens scan time or requires larger amounts of radioactivity with increased radiation dose to the animal. One also can derive the point-spread function (PSF) of the pinhole aperture, so that the pinhole geometry can be modeled in the reconstruction algorithm, with the goal of minimizing the effect of blurring in the final reconstructed image.[5]

Additional blurring that degrades SPECT resolution can be caused by the finite thickness of the γ-ray detector, especially when the photon strikes the detector surface at an oblique direction, so that the interaction coordinates in the plane parallel to the detector surface differs from the point where the photon entered the detector surface. This effect is called depth of interaction (DOI) effect, and can cause positioning errors that increase with the photon energy, incident angle and detector thickness.[6]

These two blurring effects are not shift invariant and in fact are strongly dependent on the trajectory of the photon, and therefore can be only approximated with a shift-invariant point-spread

function. For this reason, a more accurate model is desirable to compensate for these effects in image reconstruction. Since SPECT imaging naturally involves photon-matter interactions, a realistic Monte Carlo based photon transport model can give an accurate description and correction for both effects. This paper presents an accurate Monte Carlo model of pinhole blurring and DOI effects. We also describe an efficient approach for improving the spatial resolution and detection efficiency tradeoff by incorporating these effects in the image reconstruction algorithm.

2. METHODS

2.1. Monte Carlo Based Reconstruction Algorithm

The SPECT imaging process can be described as a matrix operation:

$$P = M \cdot X \tag{1}$$

where X is the radionuclide distribution (or "image"), and P the projection data measured with the imaging system. M is a system matrix that maps the 3-dimensional radionuclide distribution into the 2-dimensional projection data acquired over multiple angles. The system matrix M contains all of the geometrical information and the effects of physical processes. Image reconstruction algorithm thus requires a solution to the inverse problem, *i.e.*, calculating the unknown X from the measured quantity P. Clearly, the more accurate knowledge we have about M, the more accurately we can derive the image X.

Although from Eq. 1 one could think of inverting M directly to obtain X, this is extremely difficult due to the enormous size of M and the ill-conditioned nature of the equation.[7] Rather, the reconstruction is commonly performed with either analytical or iterative methods.[8] One of the most widely adapted algorithms is the Maximum Likelihood Expectation Maximization (ML-EM), which models Poisson noise and obtains incremental improvements through an iterative process: [9]

$$f_b^{(n+1)} = f_b^{\,n} \frac{1}{\sum_d^D p_{bd}} \sum_d^D \frac{n_d \, p_{bd}}{\sum_{b'}^B f_{b'}^{\,n} \, p_{b'd}} \tag{2}$$

where f_b is the unknown radionuclide distribution, and n_d - the recorded projection values. The system matrix $M = \{p_{bd}\}$ thereby relates the distribution $X = \{f_b\}$ with the projection $P = \{n_d\}$ according to Eq. 1. Because of the large size of M, the values of p_{bd} generally are not calculated explicitly but can be computed from a set of precalculated and stored PSFs.[10] As mentioned above, this can introduce approximations and inaccuracies into the final reconstructed image. On the other hand, the values of p_{bd} can be obtained with better accuracy using Monte Carlo methods to perform stochastic modeling of the photon imaging process in terms of accurate simulation of photon interactions, more realistic representation of the imaging geometry and the pinhole collimator geometry, and the detector response. Thus, the idea of Monte Carlo based reconstruction is to obtain the matrix M using Monte Carlo modeling and apply it to Eqs. 1 and 2 to improve the quality of the final reconstructed images.

2.2. Monte Carlo Simulation Model

Realistic models of a lead pinhole collimator, and a γ-ray detector made from cadmium zinc telluride (CdZnTe), were based on a SPECT/CT dual-modality scanner developed at UCSF[11] (Figure 1). The simulation model and associated software were designed and developed to simulate the geometrical and septal penetration effect of the pinhole and the DOI effects in the detector.

The simulation included the following simplified steps:

1) a photon with unit weight is generated with random position and direction based on a uniform distribution in the entire field of view (FOV) of the system, a space that is visible by the collimated detector over all the projection angles;

2) the photons with the appropriate trajectories are transported through the pinhole to calculate their density distribution multiplied by the probability of penetration; and

3) the photons passing through the pinhole then are used to calculate the associated interaction location in the detector.

Variance reduction techniques including angular weighting have been applied to increase computational speed, and scatter interactions have been ignored for simplicity. A set of equations describing the pinhole geometry are pre-solved using Mathematica (Wolfram Research, Inc) then used in the simulation code for photon transport in the pinhole region to accelerate the calculation of surface crossing points, with the results of the Monte Carlo simulation stored in an optimized, compact list table for fast access and minimal storage space.

2.3. Evaluation – Simulations and Experiments

The Monte Carlo based reconstruction method was evaluated by generating both simulated and experimental data for various pinhole collimators having aperture diameters ranging from 1 to 4 mm. Both simulated and experimental data used an 80×80 CdZnTe solid-state detector having a size of $20\times20\times0.5$ cm^3 with 2.5×2.5 mm^2 pixel pitch (Fig. 1).

The simulated data were obtained with a pinhole-detector distance of 21.2 cm, and a pinhole-object distance of 3.5 cm, to give a FOV with a 3 cm diameter for imaging mice. A numerical resolution phantom with hot spots ranging from 1.1 to 1.6 mm in diameter and spacing was centered in the FOV to generate noise-free projections. The system matrix corresponding to this pinhole and detector configuration was obtained by Monte Carlo simulation.

Projections were then reconstructed using an ML-EM algorithm (Eq. 2) with the Monte Carlo derived system matrix. Twenty iterations were used for reconstructing images obtained with an ideal pinhole, while 2000 iterations were used to reconstruct data obtained with the 4 mm pinhole. Modulation transfer functions (MTF) at those pinhole diameters also were calculated from the reconstructed images of simulated data obtained from a fine line source.

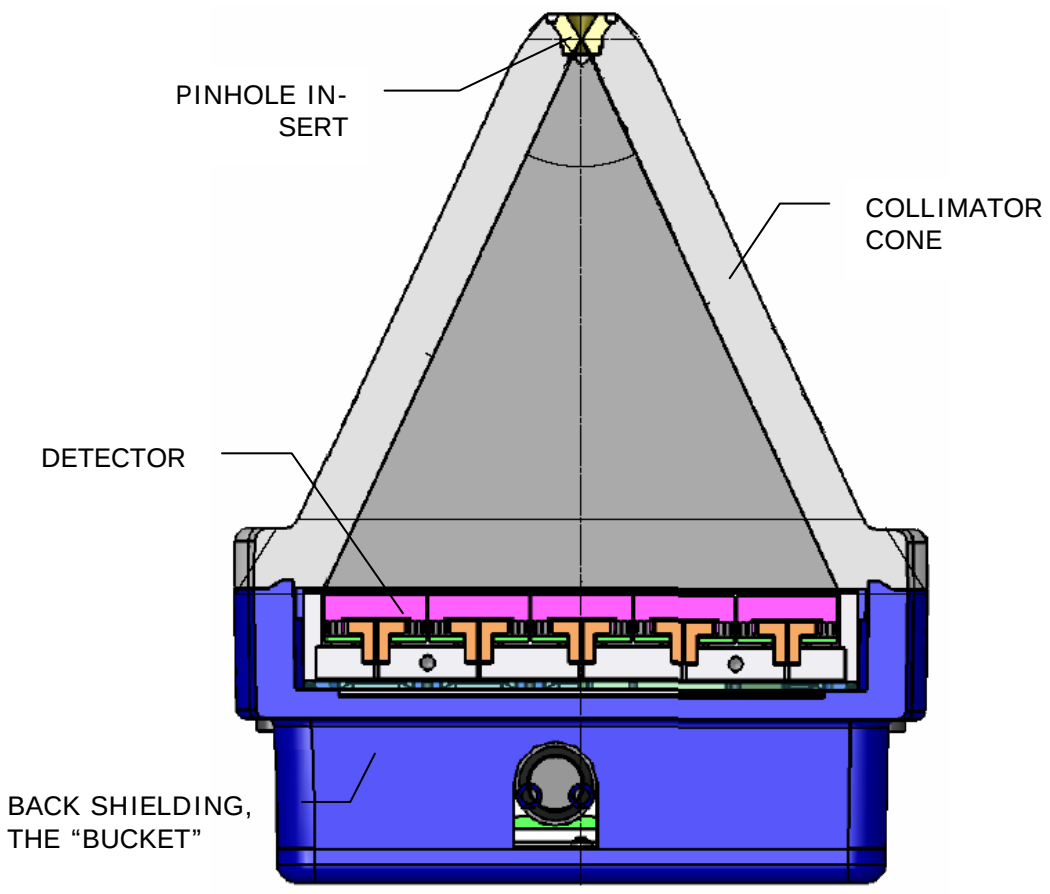

Figure 1. The detector shielding, including a collimator cone in front of the detector and a lead housing at the sides and the back.

Experimental data were acquired with a small animal SPECT/CT scanner developed at UCSF, with a pinhole-detector distance of 21.2 cm and a pinhole-object distance 4.5 cm for a FOV of 3.8 cm. Projection data were recorded of a resolution phantom filled with Tc-99m (photon energy of 140 keV), with hot spots ranging from 1.2 to 1.7 mm in diameter and spacing. The SPECT projection data were acquired with 6 million counts recorded in the energy window. Images were reconstructed as an 80×80×80 array, with 300 iterations for data from the 2 mm diameter pinhole and 1800 iterations for data recorded with the 4 mm diameter pinhole. For comparison, the same experimental data were also reconstructed with ML-EM without collimator and detector response compensation.

Experimental data with small animals were also taken and reconstructed. In a renal perfusion study, a rabbit was sacrificed and one of its kidneys containing 200 μCi of ^{99m}Tc-sestamibi was imaged with a 4 mm pinhole at 5.9 cm radius of rotation and 29 cm of detector-to-pinhole distance. Sixty projections were taken at 30 seconds each. Images were reconstructed with 1800 iterations. *In vivo* mouse imaging was also done and resultant images shown.

3. RESULTS

The Monte Carlo model based reconstruction produced MTFs similar for all pinholes with different diameters ranging from 1 to 4 mm. Although the number of iterations required for different pinhole geometries varies widely, the magnitudes of the MTFs obtained all reached ~ 80% at 1.3 mm^{-1}. Figure 2 shows the MTF from the simulated fine line source with a 4 mm pinhole and the aforementioned detector and configuration, using the model-based reconstruction with 400 iterations. This similarity in MTFs (and in spatial responses) for different pinhole geometries demonstrates that the resolution degradation due to the finite pinhole diameter could be recovered by carefully modeling the imaging geometry and photon transmission and penetration, and by incorporating this information into image reconstruction.

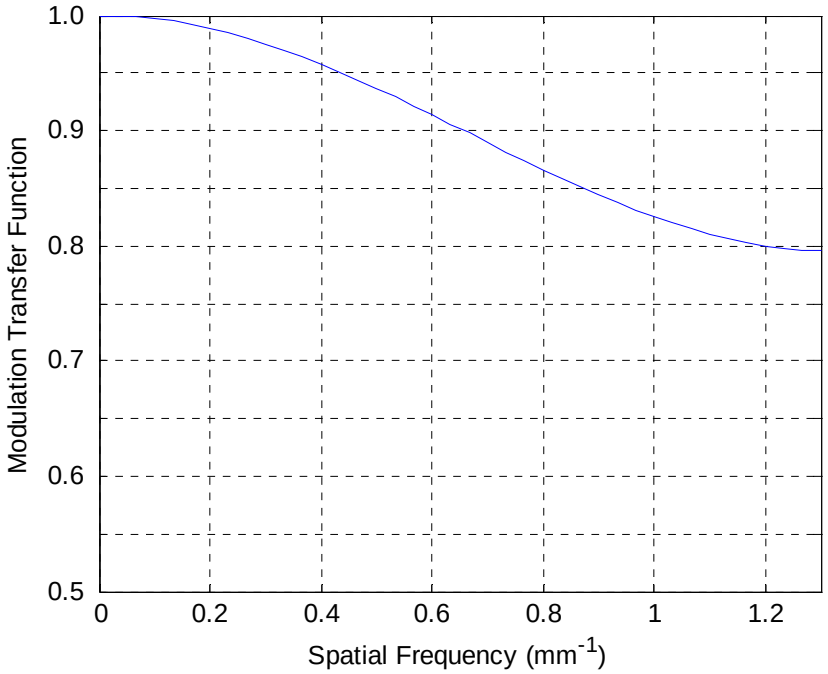

Figure 2. The modulation transfer function of the MC-based reconstruction from a 4 mm pinhole after reconstruction with 400 iterations.

This is evident in the resolution phantom studies. The simulated phantom data (Fig. 3) showed excellent reconstructions with this Monte Carlo based reconstruction method, with all the hot spots being resolved clearly. The experimental phantom data (Fig. 4) also were reconstructed with all sections of the resolution phantom visible. However, without collimator and detector response modeling, the reconstruction algorithm produced blurry images with no individual spots distinguishable for spots diameters smaller than 1.4 mm with the 2 mm diameter pinhole, and for all spot sections with the 4 mm diameter pinhole.

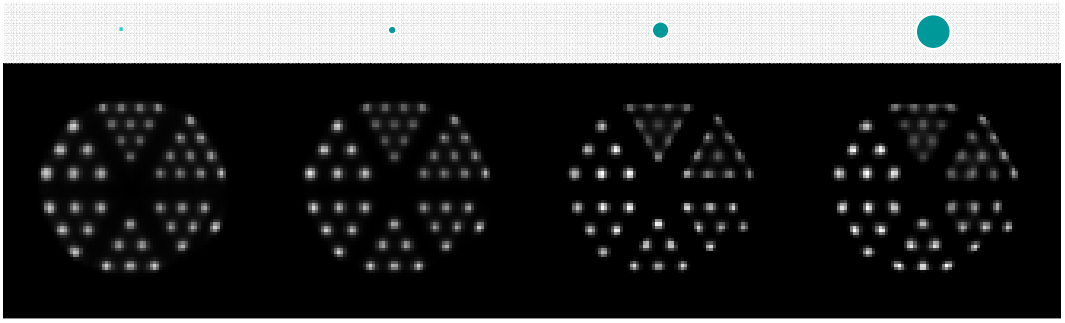

Figure 3. Reconstructed images from simulated data at different pinhole sizes. The pinholes are shown on top of the images in the proportional scale to the phantom size. The rod sizes range from 1.1 mm to 1.6 mm.

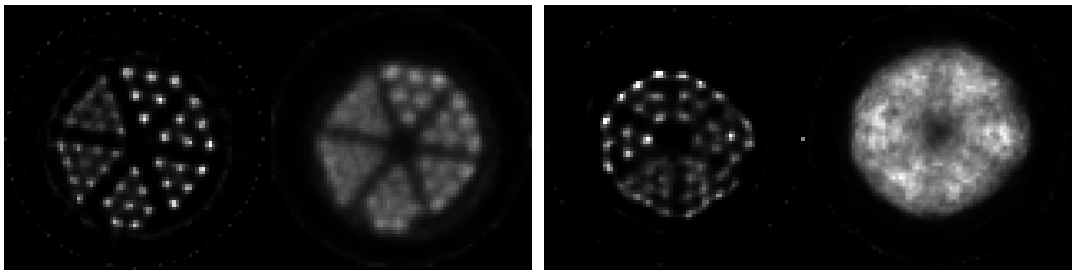

Figure 4. Reconstruction comparison. On the left is data taken with a 2 mm pinhole, reconstructed with the MC-based method and with ordinary ML-EM. On the right the data is taken with a 4 mm pinhole, again reconstructed with the MC-based method and ordinary ML-EM.

The rabbit kidney in the *ex vivo* scan contained less than 200 μCi (0.74 MBq) ^{99m}Tc, but the reconstructed slices nevertheless showed good result. Autoradiography, a gold standard, was performed for comparison purpose. As shown in Fig. 5, the coronal view of the slices from reconstruction demonstrated accumulation of ^{99m}Tc in the renal cortex. This is also shown in the autoradiographs where the cortex uptake is clearly visible. Both the SPECT scan and the autoradiography thus agree with each other well.

Figure 6 shows a mouse scan after administrated with ^{99m}Tc-sestamibi. Imaged with a 4 mm pinhole, the projection data was extremely blurry and no internal structure is distinguishable. The Monte Carlo based reconstruction, however, again improved the image quality dramatically. The image on the right in Fig. 6 is a maximum intensity projection (MIP) image of the volumetric data after reconstruction. The details have been largely restored over the original projection image on the left.

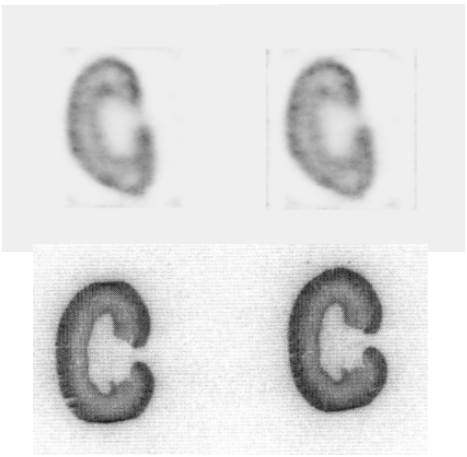

Figure 5. Reconstruction of a rabbit kidney *ex vivo* scan. In the top row are the reconstructed slices in coronal view; below them are autoradiographs from a different sample in the same batch. The SPECT data were taken in 60 frames at 30 seconds each.

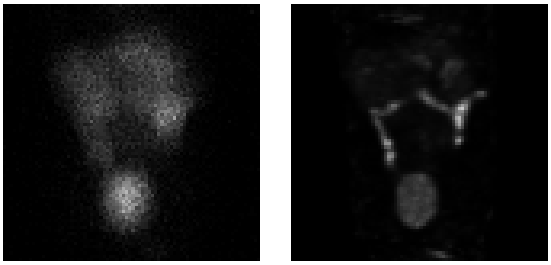

Figure 6. Image of a mouse. On the left is a projection image on the CZT detector through a 4 mm pinhole; on the right is a MIP image after being reconstructed with the MC-based method.

4. CONCLUSIONS

A Monte Carlo based system matrix and reconstruction has been efficiently implemented with an ML-EM algorithm. It is readily transferable to other iterative algorithms[8] such as OS-EM and MAP. The system matrices generated with Monte Carlo simulation can model the imaging system more faithfully than conventional techniques, with the resulting reconstructions demonstrating considerable improvement. This method will be useful especially for pinhole SPECT of small animals where the PSF is highly position dependent and difficult to calculate with high accuracy using analytical techniques.

ACKNOWLEDGMENTS

This project was supported by NIH grant R01 EB00348: "Imaging Structure and Function in Small Animals", from the National Institute of Biomedical Imaging and Bioengineering

(NIBIB). It was also partially supported by a University of California Discovery Grant bio02-10300 from the University of California Office of the President.

REFERENCES

1 S. R. Cherry, J. A. Sorenson and M. E. Phelps, *Physics in Nuclear Medicine*, 3rd ed. Saunders, Philadelphia, (2003).

2 B. H. Hasegawa, M. C. Wu, K. Iwata, A. B. Hwang, K. H. Wong, W. C. Barber, M. W. Dae and A. E. Sakdinawat, "Applications of penetrating radiation for small animal imaging", *Proceeding of the International Society for Optical Engineering*, Vol 4786, pp. 80-90, (2002).

3 M. C. Wu, B. H. Hasegawa and M. W. Dae, "Performance evaluation of a pinhole SPECT system for myocardial perfusion imaging of mice," Med Phys, **29** (12), 2830-9 (2002).

4 L. R. MacDonald, B. E. Patt, J. S. Iwanczyk, B. M. W. Tsui, Y. Wang, E. C. Frey, D. E. Wessell, P. D. Acton and H. F. Kung, "Pinhole SPECT of mice using the LumaGEM gamma camera," Nuclear Science, IEEE Transactions on, **48** (3), 830-836 (2001).

5 M. F. Smith and R. J. Jaszczak, "An analytic model of pinhole aperture penetration for 3D pinhole SPECT image reconstruction," Phys Med Biol, **43** (4), 761-75 (1998).

6 A. B. Hwang, K. Iwata and B. H. Hasegawa, "Simulation of depth of interaction effects for pinhole SPECT", *Proceeding of IEEE Nuclear Science Symposium Conference*, Piscataway, NJ, Vol 3, pp. 1293-7, (2002).

7 B. Silverman, M. Jones, J. Wilson and D. Nychka, "A smoothed EM approach to indirect estimation problem, with particular, reference to stereology and emission tomography," J R Statist Soc B, **52** (2), 271-324 (1990).

8 P. P. Bruyant, "Analytic and iterative reconstruction algorithms in SPECT," J Nucl Med, **43** (10), 1343-58 (2002).

9 L. A. Shepp and Y. Vardi, "Maximum likelihood reconstruction for emission tomography," Medical Imaging, IEEE Transactions on, **1** (2), 113-122 (1982).

10 H. Zaidi, ed. *Quantitative Analysis in Nuclear Medicine Imaging*. New York: Springer Science+Business Media, Inc., (2006).

11 T. Funk, M. Sun, A. B. Hwang, J. Carver, S. Thompson, K. B. Parnham, R. Luu, B. E. Patt, J. Li, K. Iwata and B. H. Hasegawa, "A multidetector high resolution SPECT/CT scanner with continuous scanning capability," in *Small-animal SPECT imaging*, edited by H. H. Barrett, Springer, (2005).